

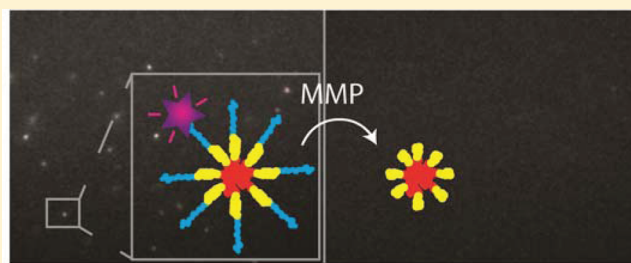
# Thermosensitive Peptide-Hybrid ABC Block Copolymers Obtained by ATRP: Synthesis, Self-Assembly, and Enzymatic Degradation

Albert J. de Graaf,<sup>†</sup> Enrico Mastrobattista,<sup>†</sup> Tina Vermonden,<sup>†</sup> Cornelus F. van Nostrum,<sup>†</sup> Dirk T. S. Rijkers,<sup>‡</sup> Rob M. J. Liskamp,<sup>‡</sup> and Wim E. Hennink<sup>\*†</sup>

<sup>†</sup>Utrecht Institute for Pharmaceutical Sciences, Pharmaceutics, Utrecht University, P.O. Box 80.082, 3508TB Utrecht, The Netherlands

<sup>‡</sup>Utrecht Institute for Pharmaceutical Sciences, Medicinal Chemistry & Chemical Biology, Utrecht University, P.O. Box 80.082, 3508TB Utrecht, The Netherlands

**ABSTRACT:** Peptide-hybrid ABC block copolymers were synthesized by growing two different polymer chains from a native peptide using atom transfer radical polymerization (ATRP). To this end, two different ATRP initiators were coupled via orthogonal methods to the N- and C-terminus of the peptide Ser-Gly-Pro-Gln-Gly-Ile-Phe-Gly-Gln-Met-Gly, a substrate for matrix metalloproteases 2 and 9. First, a hydrophilic block of poly(oligo(ethylene glycol) methyl ether methacrylate) (pOEGMA) was polymerized from the peptide's C-terminus. Before polymerization of the second block, the first living chain end was inactivated by substitution of its Cl-terminus with azide under mild conditions. Then, a thermosensitive block of poly(*N*-isopropylacrylamide) (pNIPAm) was polymerized from the peptide's N-terminus. Well-defined polymers were obtained with good control over both block sizes. The resulting polymers self-assembled into micelles above the cloud point of the pNIPAm block. As anticipated, it was shown that the peptide linkage between the polymer blocks can be cut by a metalloprotease, leading to "shedding" of the corona of the micelles which makes these systems potentially suitable for enzyme-triggered drug delivery.



## INTRODUCTION

The field of biohybrid materials (materials that consist of synthetic materials together with biomolecules or even entire cells) has been rapidly expanding over the past decade. This is due to the promises it holds for pharmaceutical, medical, and bio- and nanotechnological applications.<sup>1,2</sup> Among others, biohybrid materials are under investigation for use in targeted drug delivery and for the controlled release of therapeutic (bio)molecules. For example, biohybrid hydrogels can be used as depot formulations of drugs or as scaffolds for tissue engineering, whereas biohybrid micelles and vesicles are under investigation for targeted drug delivery to inflamed tissue, e.g., in cancer and rheumatoid arthritis.<sup>3–8</sup> In these materials, the "bio" part may e.g. be a peptide containing a cell adhesion site or an enzymatic cleavage site or a pH-, redox-, or temperature-responsive peptide.<sup>4–6</sup>

A number of techniques are presently available for the design of such peptide-hybrid polymers, including coupling a peptide to a pre-made polymer (the "grafting to" approach),<sup>9,10</sup> polymerizing a peptide-functionalized monomer (the "grafting through" approach),<sup>11,12</sup> or performing a polymerization using a peptide macroinitiator (the "grafting from" approach).<sup>13,14</sup>

The advent of several controlled, "living" radical polymerization techniques has greatly expanded the scope of these "grafting" techniques. Techniques such as atom transfer radical polymerization (ATRP),<sup>15–17</sup> reversible addition–fragmenta-

tion chain transfer (RAFT) polymerization,<sup>18–20</sup> and nitroxide-mediated polymerization (NMP)<sup>21–23</sup> allow for the synthesis of low-dispersity polymers with defined, reactive chain-ends.<sup>24</sup> A variety of monomers can be polymerized using these techniques, often under mild conditions. Furthermore, living radical polymerizations are compatible with many functional groups. Together, these properties render living radical polymerizations suitable for use in "grafting from" and "grafting through" strategies.<sup>25</sup>

In the present work we aimed at incorporating a peptide into semisynthetic amphiphilic triblock copolymers, such that the peptide is positioned between a hydrophilic and a thermosensitive block. For the hydrophilic block of the final block copolymer, oligo(ethylene glycol) methyl ether methacrylate (OEGMA,  $M_n = 300$  Da) was chosen as monomer. The thermosensitive block was prepared by polymerization of *N*-isopropylacrylamide (NIPAm). In aqueous solutions, these polymers likely self-assemble into micellar structures above the cloud point (CP) of the thermosensitive block as demonstrated for other thermosensitive block copolymers.<sup>26,27</sup> The peptide, Ser-Gly-Pro-Gln-Gly-Ile-Phe-Gly-Gln-Met-Gly, was designed to be functionalizable by specific chemistries on both its N- and C-

Received: November 8, 2011

Revised: December 26, 2011

Published: January 12, 2012

terminus. Furthermore, this peptide is cleavable at the Gly–Ile bond by matrix metalloproteinases (MMPs) 2 and 9,<sup>28</sup> which are upregulated in inflamed tissues such as in cancer and rheumatoid arthritis.<sup>29–31</sup> Micelles, formed by self-assembly of these amphiphilic block copolymers above the CP of the pNIPAM block, can be loaded with a drug and be administered intravenously. Because of the enhanced permeability and retention (EPR) effect, they will accumulate in the inflamed target tissue,<sup>32</sup> where the hydrophilic stealth corona will subsequently be selectively shed off by action of the MMPs. The exposed micellar cores may then be taken up by the target cells or aggregate and release their payload over time.<sup>33</sup>

In order to generate these thermosensitive block copolymers with a peptide connecting the hydrophilic and thermosensitive polymer blocks, in the present paper, two sequential polymerizations, each initiating on the other terminus of the same peptide, were carried out. Thereby, full benefit is taken from the advantages of the “grafting from” approach, mainly the high coupling efficiency and easy work-up. To the best of our knowledge, this is the first report of two sequential “grafting from” polymerizations, initiated from the C- and N-terminus of a peptide. Furthermore, we use the same polymerization technique, ATRP, for both blocks. At present, sequential “grafting from” has only been performed using a nonpeptide initiator carrying two initiating moieties each for a different polymerization chemistry.<sup>34,35</sup> It is shown that well-defined amphiphilic polymers can indeed be synthesized in this way. These polymers self-assemble into micelles, having a corona which can be shed off by action of a metalloprotease.

## EXPERIMENTAL PART

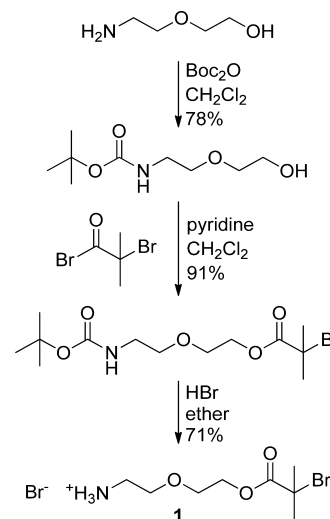
**Chemicals.** All solvents were obtained from Biosolve (Valkenswaard, The Netherlands). Unless otherwise noted, the chemicals were obtained from Sigma-Aldrich (Steinheim, Germany) and were used as received. Prior to use, *N,N*-dimethylacetamide (DMA) was dried on calcium hydride, distilled under reduced pressure, and stored over 4 Å molecular sieves. Triethylamine was dried on potassium hydroxide, distilled, and stored on 3 Å molecular sieves. Oligo(ethylene glycol) methyl ether methacrylate with average  $M_n$  of 300 Da (OEGMA<sub>300</sub>) was passed over a column of basic alumina immediately prior to use. Tris[2-(dimethylamino)ethyl]amine (Me<sub>6</sub>TREN) was prepared and purified according to a literature procedure.<sup>36</sup>

**Analytical Methods.** HPLC was performed on a Waters 2695 system equipped with a dual wavelength UV absorption detector set to 210 and 254 nm. An Alltech ProSper C18 column was used at 25 °C, employing a gradient of CH<sub>3</sub>CN/H<sub>2</sub>O/TFA 5/95/0.1 to 60/40/0.1 in 1 h. Unless noted otherwise, gel permeation chromatography (GPC) was performed on a Waters 2695 system equipped with a differential refractive index detector using a MixedD column (Polymer laboratories). The column temperature was 40 °C, 10 mM LiCl in DMF was used as the eluent at a flow rate of 1 mL/min, and linear PEG standards were used for calibration. Samples were allowed to dissolve for at least 16 h prior to analysis.

NMR spectra were recorded on a Varian Mercury spectrometer operating at 300 MHz (<sup>1</sup>H) or 75.5 MHz (<sup>13</sup>C), and ESI-MS spectra were recorded on a Shimadzu QP8000 mass spectrometer. MALDI-TOF MS was performed on a Kratos Axima CFR apparatus using ACTH as external standard and  $\alpha$ -cyano-4-hydroxycinnamic acid as matrix.

**Synthesis of 2-(2-Aminoethoxy)ethyl-2-bromoisobutyrate Hydrobromide (Linker 1).** The synthesis of linker 1 is shown in Scheme 1. In a round-bottom flask, 2-(2-aminoethoxy)ethanol (11.0 mL, 110 mmol) and di-*tert*-butyl dicarbonate (21.8 g, 100 mmol) were dissolved in CH<sub>2</sub>Cl<sub>2</sub> (100 mL). The resulting mixture was stirred 16 h at room temperature. Then, the mixture was washed three times with 1 M NaHSO<sub>4</sub>, three times with saturated NaHCO<sub>3</sub>, and once with

**Scheme 1. Synthesis Route of 2-(2-Aminoethoxy)ethyl-2-bromoisobutyrate Hydrobromide (Linker 1)**

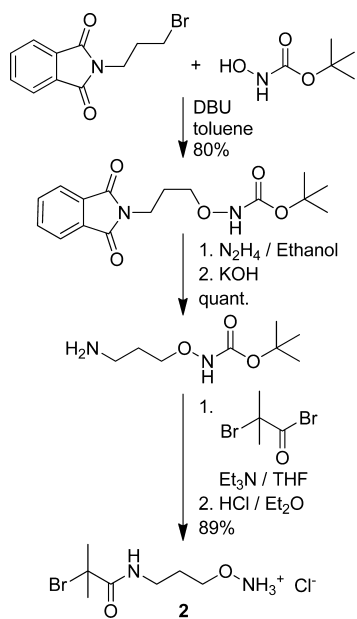


saturated NaCl. After drying on anhydrous MgSO<sub>4</sub>, the CH<sub>2</sub>Cl<sub>2</sub> layer was evaporated *in vacuo*, giving 2-(*N*-Boc-2-aminoethoxy)ethanol as a colorless oil in 78% yield (15.9 g, 78 mmol). <sup>1</sup>H NMR (300 MHz, CDCl<sub>3</sub>):  $\delta$  5.28 (bs, 1H), 3.66 (t, 2H), 3.50 (t, 2H), 3.48 (t, 2H), 3.25 (m, 2H), 3.10 (bs, 1H), 1.37 (s, 9H). <sup>13</sup>C NMR (75.5 MHz, CDCl<sub>3</sub>):  $\delta$  156.3 (C=O), 79.4 (C(CH<sub>3</sub>)<sub>3</sub>), 72.3 (CH<sub>2</sub>), 70.3 (CH<sub>2</sub>), 61.5 (CH<sub>2</sub>), 40.4 (CH<sub>2</sub>), 28.4 (CH<sub>3</sub>).

In the next reaction step, 2-(*N*-Boc-2-aminoethoxy)ethanol (14.3 g, 70 mmol) and pyridine (6.2 mL, 77 mmol) were dissolved in anhydrous CH<sub>2</sub>Cl<sub>2</sub> (100 mL), and the solution was cooled on an ice bath. To this solution, 2-bromoisobutyryl bromide (9.5 mL, 77 mmol) was added dropwise while stirring. After addition, the mixture was allowed to reach room temperature and stirred for 30 min. The precipitated pyridinium bromide was filtered off. The filtrate was washed three times with 1 M NaHSO<sub>4</sub>, three times with saturated NaHCO<sub>3</sub>, and one time with saturated NaCl. After drying on anhydrous MgSO<sub>4</sub>, the CH<sub>2</sub>Cl<sub>2</sub> layer was evaporated *in vacuo*, giving 2-(*N*-Boc-2-aminoethoxy)ethyl-2-bromoisobutyrate in 91% yield (24.4 g, 69 mmol). The product was a colorless oil which slowly crystallized upon standing. <sup>1</sup>H NMR (300 MHz, CDCl<sub>3</sub>):  $\delta$  4.93 (bs, 1H), 4.30 (t, 2H), 3.68 (t, 2H), 3.53 (t, 2H), 3.28 (m, 2H), 1.92 (s, 6H), 1.41 (s, 9H). <sup>13</sup>C NMR (75.5 MHz, CDCl<sub>3</sub>):  $\delta$  171.8 (C=O), 156.1 (C=O), 79.4 (C(CH<sub>3</sub>)<sub>3</sub>), 70.3 (CH<sub>2</sub>), 68.6 (CH<sub>2</sub>), 65.0 (CH<sub>2</sub>), 55.7 (C–Br), 40.4 (CH<sub>2</sub>), 30.9 (C(CH<sub>3</sub>)<sub>2</sub>), 28.5 (C(CH<sub>3</sub>)<sub>3</sub>).

In the last reaction step, 2-(*N*-Boc-2-aminoethoxy)ethyl-2-bromoisobutyrate (24 g, 68 mmol) was dissolved in diethyl ether (200 mL), and HBr (28 mL of a 33% solution in acetic acid) was added dropwise, after which the product precipitated out of solution. The reaction was left at room temperature for 16 h. The resulting white crystals of 2-(2-aminoethoxy)ethyl-2-bromoisobutyrate (**1**) were harvested by filtration, washed three times with a small volume of diethyl ether, and dried *in vacuo*. Yield: 16.1 g (48 mmol, 71%). <sup>1</sup>H NMR (300 MHz, CDCl<sub>3</sub>):  $\delta$  7.93 (bs, 3H), 4.39 (t, 2H), 3.89 (t, 2H), 3.81 (t, 2H), 3.32 (m, 2H), 1.94 (s, 6H). <sup>13</sup>C NMR (75.5 MHz, CDCl<sub>3</sub>):  $\delta$  171.9 (C=O), 69.0 (CH<sub>2</sub>), 66.5 (CH<sub>2</sub>), 65.1 (CH<sub>2</sub>), 56.0 (C–Br), 40.0 (CH<sub>2</sub>), 30.9 (C(CH<sub>3</sub>)<sub>2</sub>). ESI-MS: calcd for C<sub>8</sub>H<sub>17</sub>NO<sub>3</sub>Br [M]<sup>+</sup> 254.04; found 254.25.

**Synthesis of *N*-(3-Aminoxypropyl)-2-bromo-2-methylpropionylamide Hydrochloride (Linker 2).** The synthesis of linker 2 is shown in Scheme 2. In a round-bottom flask, *N*-3-bromopropylphthalimide (24.5 g, 91 mmol) and *N*-Boc-hydroxylamine (13.3 g, 100 mmol) were dissolved in toluene (100 mL). The solution was boiled under reflux, and 1,8-diazabicyclo[5.4.0]undec-7-ene (DBU) (15 mL, 100 mmol) was added dropwise. During the addition of DBU the desired product separated as a yellow oil. After stirring for 1 h, the mixture was concentrated *in vacuo*. The residue was redissolved in

**Scheme 2. Synthesis Route of *N*-(3-Aminoxypropyl)-2-bromo-2-methylpropionylamide Hydrochloride (Linker 2)**


$\text{CH}_2\text{Cl}_2$  (200 mL) and washed with 10% citric acid ( $4 \times 50$  mL).<sup>37</sup> The organic phase was dried over  $\text{MgSO}_4$  and concentrated *in vacuo* to give *N*-(3-(*N*-Boc-aminoxy)propyl)phthalimide as a pale yellow solid in 80% yield (23.5 g, 73 mmol).  $^1\text{H}$  NMR (300 MHz,  $\text{CDCl}_3$ ):  $\delta$  7.85 (t, 2H), 7.72 (t, 2H), 7.35 (s, 1H), 3.94 (t, 2H), 3.84 (t, 2H), 2.02 (m, 2H), 1.48 (s, 9H).  $^{13}\text{C}$  NMR (75.5 MHz,  $\text{CDCl}_3$ ):  $\delta$  168.5 (imide C=O), 157.0 (urethane C=O), 134.1 (CH), 132.2 (C), 123.3 (CH), 81.8 ( $\underline{\text{C}}(\text{CH}_3)_3$ ), 74.0 ( $\text{CH}_2$ ), 35.1 ( $\text{CH}_2$ ), 28.3 ( $\underline{\text{C}}(\text{CH}_3)_3$ ), 27.3 ( $\text{CH}_2$ ).

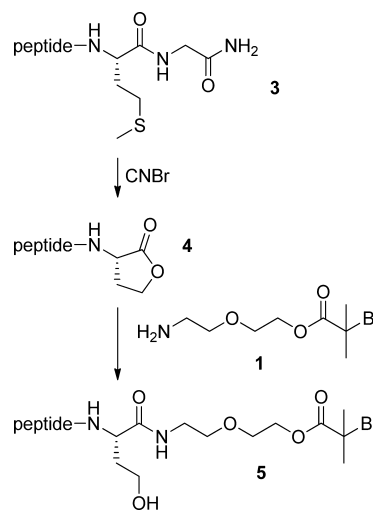
In the next step, *N*-(3-(*N*-Boc-aminoxy)propyl)phthalimide (13 g, 40 mmol) was dissolved in absolute ethanol (50 mL). Hydrazine hydrate (3 mL of an 85% aqueous solution) was added dropwise, and the mixture was boiled under reflux for 2 h. The product separated as its salt with phthalylhydrazide, from which it was liberated by adding KOH (2.5 g dissolved in 20 mL of absolute ethanol). After stirring vigorously for 1 h, the precipitate had turned into a fine white powder, the potassium salt of phthalylhydrazide. The mixture was concentrated *in vacuo*, resuspended in anhydrous  $\text{CHCl}_3$  (100 mL) under vigorous stirring for 1 h, and filtered. The solids were washed three times with a small amount of  $\text{CHCl}_3$ . The combined filtrates were dried on  $\text{MgSO}_4$  and concentrated *in vacuo* to give 3-(*N*-Boc-aminoxy)propylamine as an oil in quantitative yield (8 g, 40 mmol).  $^1\text{H}$  NMR (300 MHz,  $\text{CDCl}_3$ ):  $\delta$  3.93 (t, 2H), 3.84 (t, 2H), 1.96 (bs, 2H), 1.75 (m, 2H), 1.46 (s, 9H).  $^{13}\text{C}$  NMR (75.5 MHz,  $\text{CDCl}_3$ ):  $\delta$  157.5 (C=O), 82.0 ( $\underline{\text{C}}(\text{CH}_3)_3$ ), 75.0 ( $\text{CH}_2$ ), 39.1 ( $\text{CH}_2$ ), 29.4 ( $\text{CH}_2$ ), 28.4 ( $\underline{\text{C}}(\text{CH}_3)_3$ ). ESI-MS: calcd for  $\text{C}_8\text{H}_{19}\text{N}_2\text{O}_3$  [ $\text{M} + \text{H}$ ] $^+$ : 191.14; found 190.90.

Subsequently, 3-(*N*-Boc-aminoxy)propylamine (6.9 g, 36 mmol) and triethylamine (7.5 mL, 54 mmol) were dissolved in anhydrous THF (70 mL). The mixture was purged with  $\text{N}_2$  and cooled on an ice bath, after which 2-bromoisobutyryl bromide (6.7 mL, 54 mmol) was added dropwise while stirring. Next, the ice bath was removed, and the mixture was stirred for 1 h at room temperature. The precipitated triethylammonium bromide was filtered off, and the filtrate was concentrated *in vacuo*. The residue was redissolved in EtOAc (300 mL), and this solution was washed with 1 M  $\text{NaHSO}_4$  ( $3 \times 50$  mL), 1 M  $\text{NaHCO}_3$  ( $3 \times 50$  mL), and saturated NaCl ( $2 \times 50$  mL). The organic layer was dried on  $\text{MgSO}_4$  and concentrated *in vacuo* to give *N*-(3-(*N*-Boc-aminoxy)propyl)-2-bromo-2-methylpropionylamide as a yellow oil. A fraction (8 g) of this oil was dissolved in  $\text{Et}_2\text{O}$  (25 mL), and the solution was cooled on ice. HCl gas was bubbled through the solution, upon which a white precipitate of *N*-(3-aminoxypropyl)-2-bromo-2-methylpropionylamide hydrochloride (**2**) was formed. The product was purified twice by trituration with  $\text{CH}_2\text{Cl}_2$  and  $\text{Et}_2\text{O}$  at

$-20$  °C. Yield: 4.4 g (16 mmol, 89% over two steps).  $^1\text{H}$  NMR (300 MHz,  $\text{DMSO}-d_6$ ):  $\delta$  10.92 (bs, 3H), 8.18 (t, 1H), 4.01 (t, 2H), 3.17 (q, 2H), 1.87 (s, 6H), 1.75 (m, 2H).  $^{13}\text{C}$  NMR (75.5 MHz,  $\text{DMSO}-d_6$ ):  $\delta$  170.8 (C=O), 72.0 ( $\text{CH}_2$ ), 60.7 (C-Br), 35.9 ( $\text{CH}_2$ ), 31.1 ( $\underline{\text{C}}(\text{CH}_3)_2$ ), 27.2 ( $\text{CH}_2$ ). ESI-MS: calcd for  $\text{C}_7\text{H}_{16}\text{N}_2\text{O}_2\text{Br}$  ([ $\text{M}$ ] $^+$ ): 239.04; found 238.95.

**Peptide Synthesis.** The peptide H-Ser-Gly-Pro-Gln-Gly-Ile-Phe-Gly-Gln-Met-Gly- $\text{NH}_2$  was synthesized by standard Fmoc solid phase peptide synthesis.<sup>38</sup> 350 mg of peptide (TFA salt, 0.30 mmol) was obtained, with a purity of >95% (HPLC). MALDI-TOF MS: calcd 1077.23 ([ $\text{M} + \text{H}$ ] $^+$ ); found 1077.21. The product was used without further purification.

**Functionalization of Peptide C-Terminus.** To introduce a homoserine lactone functionality at the C-terminus (Scheme 3),<sup>39–41</sup>

**Scheme 3. Functionalization of the Peptide C-Terminus with Linker 1<sup>a</sup>**


<sup>a</sup>“Peptide” indicates the sequence H-Ser-Gly-Pro-Gln-Gly-Ile-Phe-Gly-Gln-.

the peptide **3** (343 mg) was dissolved in 150 mL of  $\text{N}_2$ -flushed  $\text{CH}_3\text{CN}/\text{H}_2\text{O}/\text{TFA}$  (30/70/1). Under a nitrogen atmosphere,  $\text{CNBr}$  (12 mL of a 4 M solution in  $\text{CH}_3\text{CN}$ ) was added, and the reaction mixture was stirred for 16 h in the dark. The mixture was evaporated to dryness *in vacuo* at 28 °C. The lactone-functionalized peptide **4** was then redissolved in  $\text{CH}_3\text{CN}/\text{H}_2\text{O}/\text{TFA}$  (30/70/0.1) and lyophilized. The yield after lyophilization was 383 mg. ESI-MS: calcd 973.47 ([ $\text{M} + \text{H}$ ] $^+$ ); found 973.47.

Linker **1** (3.0 g, 0.9 mmol) was dissolved in  $\text{CH}_2\text{Cl}_2$  (50 mL) and converted into the free amine by shaking with an equimolar amount of aqueous NaOH (9.0 mL, 1.0 M). The organic layer was dried on  $\text{MgSO}_4$ , followed by evaporation of the volatiles. Directly afterward, 1.2 mL of the resulting oil was added to the homoserine lactone-functionalized peptide **4** (325 mg, 0.30 mmol) together with 2-hydroxypyridine (200  $\mu\text{L}$  of a 30 mg/mL solution in DMA). After vigorous stirring for 15 min, the reaction mixture became homogeneous, and it was then stirred for another 15 min. Excess linker and DMA were removed by precipitation of the product in MTBE (250 mL) containing 1% TFA. The resulting peptide macroinitiator **5** was purified by preparative HPLC (SunFire C18 preparative column, gradient:  $\text{CH}_3\text{CN}/\text{H}_2\text{O}/\text{TFA}$  30/70/0.1 to 50/50/0.1, over 15 min) and subsequently lyophilized yielding 294 mg (0.22 mmol) of the TFA salt of the pure peptide macroinitiator **5** as a white powder. ESI-MS: calcd 1226.51 ([ $\text{M} + \text{H}$ ] $^+$ ); found 1226.30.

**ATRP of the C-Terminal Polymer Block.** Prior to use, all solvents and liquid reagents were deoxygenated by flushing with nitrogen gas for 15 min. A catalyst stock was prepared by weighing  $\text{CuCl}$  (12.0 mg, 120  $\mu\text{mol}$ ),  $\text{CuCl}_2 \cdot 2\text{H}_2\text{O}$  (13.6 mg, 80  $\mu\text{mol}$ ), and 2,2'-bipyridyl (bpy) (62.4 mg, 400  $\mu\text{mol}$ ) into a 7 mL glass screw-

capped vial equipped with a micro stirring bar. The vial was sealed with a septum and flushed with nitrogen gas for 15 min. Then, CH<sub>3</sub>CN (0.6 mL) and H<sub>2</sub>O (1.4 mL) were added through the septum, and the vial was held in an ultrasonic bath until all solids had dissolved forming the brown catalytic complex.

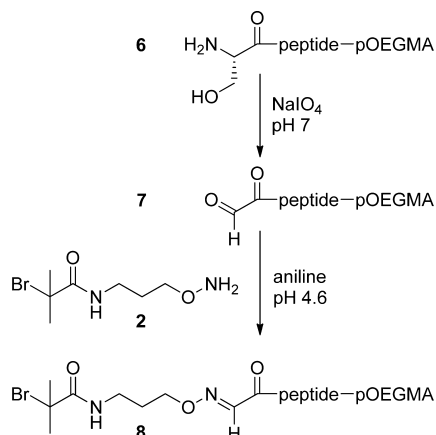
OEGMA<sub>300</sub> monomer (160, 320, or 640  $\mu$ L for the aimed pOEGMA block lengths of 4, 8, and 16 kDa, respectively) was charged into an N<sub>2</sub>-filled 2 mL septum vial equipped with a stirring bar. Then, 500  $\mu$ L of the catalyst stock solution was added, followed by the peptide macroinitiator **5** (40  $\mu$ mol, dissolved in a minimal volume of DMSO). Conversion was monitored during the reaction by <sup>1</sup>H NMR of samples diluted in air-saturated D<sub>2</sub>O, comparing the integral of the region between 6.3 and 5.6 ppm (2H, H<sub>2</sub>C=C) with the integral of the region between 4.5 and 4.0 ppm (2H, C(=O)OCH<sub>2</sub>). Furthermore, at several time points samples were taken, which were quenched by diluting in air-saturated DMF, and the evolution of molecular weight was analyzed by GPC.

**Azide Substitution of the Living Chain End.** When the monomer conversion was above 90%, NaN<sub>3</sub> (80  $\mu$ L of an N<sub>2</sub>-purged 1 M aqueous solution) was added to the reaction mixture, causing the chloride chain end to be substituted by an azide by means of the copper–bipyridyl catalyst.<sup>42</sup> Since the azide-functionalized chain end does not reinitiate, further OEGMA polymerization was prevented by this procedure. Azide functionalization also allows conjugation with a fluorescent probe.<sup>42</sup> The reaction mixture was left for 16 h to ensure complete substitution, after which the polymer was purified by 3 $\times$  10-fold concentration using a Vivaspin concentrator (MWCO of 2, 5, or 10 kDa for pOEGMA block lengths of 4, 8, and 16 kDa, respectively), each time diluting with 10 mM phosphate buffer, pH 7.0. The molecular weight of the polymers was determined by <sup>1</sup>H NMR based upon the ratio of the integrals of the aromatic phenylalanine protons and methoxy protons from pOEGMA.

**Chain Extension Experiment.** A sample (10  $\mu$ L) of the peptide-pOEGMA<sub>4 kDa</sub> polymer solution was taken before and after the substitution with NaN<sub>3</sub>. The samples were diluted with CH<sub>3</sub>CN (300  $\mu$ L) and H<sub>2</sub>O (700  $\mu$ L) in a 2 mL septum vial. Subsequently, NIPAm (18 mg for target  $M_n$  = 32 kDa), CuBr (1.8 mg), and CuBr<sub>2</sub> (1.9 mg) were added. The vial was placed in an ice bath and purged with N<sub>2</sub> for 15 min. Then, the reaction was started by adding Me<sub>6</sub>TREN (50  $\mu$ L of a 0.4 M N<sub>2</sub>-purged aqueous solution).

**Functionalization of the N-Terminus.** To introduce an aldehyde functionality at the peptide's N-terminus (Scheme 4), 60  $\mu$ L of a 1 M

#### Scheme 4. Functionalization of the Peptide N-Terminus with Linker 2<sup>a</sup>



<sup>a</sup>“Peptide” indicates the sequence -Gly-Pro-Gln-Gly-Ile-Phe-Gly-Gln-

aqueous solution of NaIO<sub>4</sub> was added to the solution of peptide-pOEGMA **6** (40 mM in 1 mL of 10 mM phosphate buffer pH 7.4). Before and 15 min after addition, samples were taken for analysis. Disappearance of the amino group was confirmed by reaction with

fluorescamine: 1  $\mu$ L of sample was diluted in 1 mL of 50 mM phosphate buffer of pH 8.9. Subsequently, to 150  $\mu$ L of this solution was added 50  $\mu$ L of a freshly prepared 0.3 mg/mL solution of fluorescamine in dry acetone. The fluorescence was recorded ( $\lambda_{\text{ex}}$  = 380 nm,  $\lambda_{\text{em}}$  = 460 nm) in a FluoStar Optima well plate reader (BMG Labtech), and it was verified that after reaction with NaIO<sub>4</sub> no fluorescence was observable. To test for the development of an aldehyde functionality, a drop of sample was placed on a TLC plate and allowed to dry. The plate was then sprayed with a solution of 2.0 g of 2,4-dinitrophenylhydrazine and 4.0 mL of concentrated sulfuric acid in 100 mL of methanol. The development of a yellow spot indicated the formation of an aldehyde **7**.

After reaction with NaIO<sub>4</sub>, the solution was diluted to 10 mL in 50 mM anilinium acetate buffer, pH 4.6.<sup>43</sup> Linker **2** (110 mg, 0.4 mmol) was added, and the reaction was allowed to proceed for 16 h at room temperature under nitrogen.

The polymer solution was again concentrated (4 $\times$  10-fold) using a Vivaspin concentrator (MWCO 2, 5, and 10 kDa), exchanging the buffer solution for demineralized water. The efficiency of coupling was assessed by <sup>1</sup>H NMR spectroscopy, comparing the integral of the proton on the oxime carbon of **8**, at 7.7 ppm, with the integral of the aromatic phenylalanine protons.

**ATRP of the N-Terminal Polymer Block.** Following a published procedure,<sup>44</sup> CuBr (1.8 mg), CuBr<sub>2</sub> (1.9 mg), and *N*-isopropylacrylamide (NIPAm) (320 or 640 mg for a target  $M_n$  of 16 and 32 kDa, respectively) were weighed into a 2 mL septum vial. A stirring bar, CH<sub>3</sub>CN (250  $\mu$ L) and the N-terminally functionalized peptide-pOEGMA **8** (1 mL of a 20 mM aqueous solution) were added. For the target  $M_n$  of 32 kDa, it was necessary to add 1 extra mL of H<sub>2</sub>O and 250  $\mu$ L of CH<sub>3</sub>CN to dissolve the NIPAm. The vial was placed in an ice bath, and the solution was purged with N<sub>2</sub> for 15 min. Then, the reaction was started by adding 50  $\mu$ L of a 0.4 M N<sub>2</sub>-purged aqueous solution of Me<sub>6</sub>TREN. During the reaction, the conversion was monitored by <sup>1</sup>H NMR of samples diluted in air-saturated D<sub>2</sub>O. Furthermore, at several time points samples were taken, which were quenched by diluting in air-saturated DMF and analyzed by gel permeation chromatography (GPC). The final polymers were dialyzed against water and lyophilized.

**Polymer Characterization.** CPs of the polymers were determined using a Shimadzu UV-2450 spectrophotometer with temperature control by a Peltier element. The temperature of polymer solutions (1 mg/mL) was raised from 20 to 50 at 1  $^{\circ}$ C/min, and the CP was defined as the onset of the curve of extinction at 650 nm vs temperature.

For the determination of the critical micelle concentration (cmc), the different block copolymers were dissolved in water in concentrations ranging from 1  $\mu$ g/mL to 1 mg/mL. Then, 5  $\mu$ L of a 1.8  $\times$  10<sup>-4</sup> M solution of pyrene in acetone was added to 1 mL of polymer solution. The micelles were formed by rapidly heating the solutions to 40  $^{\circ}$ C. After incubation for 16 h at this temperature, pyrene fluorescence was measured using a Horiba Fluorolog fluorometer at 37  $^{\circ}$ C. The emission was measured at 390 nm using excitation wavelengths of 333 and 338 nm. The ratio  $I_{338}/I_{333}$  was plotted against the logarithmic polymer concentration to determine the cmc.<sup>45</sup>

**Formation of Micelles.** Micelles were formed using a heat shock procedure according to Neradovic et al.<sup>46</sup> by heating 900  $\mu$ L of 0.22  $\mu$ m-filtered water or phosphate buffered saline (PBS) to 40  $^{\circ}$ C and then adding 100  $\mu$ L of a 1 mg/mL solution (at room temperature) of the polymer. The mixture was kept at 40  $^{\circ}$ C for 5 min before being equilibrated at 37  $^{\circ}$ C. Particle size was measured at 37  $^{\circ}$ C by dynamic light scattering (DLS) on an ALV CGS-3 system at a 90 $^{\circ}$  scattering angle.

**Fluorescent Labeling of the Polymer.** To 1 mL of a 10 mg/mL aqueous solution of pNIPAm<sub>32 kDa</sub>-peptide-pOEGMA<sub>8 kDa</sub> was added 3  $\mu$ L of 0.1 mM copper(II) sulfate, 15  $\mu$ L of 1 mg/mL Alexa Fluor 555 functionalized with an alkyne moiety in DMSO (Invitrogen), and 30  $\mu$ L of 0.1 M ascorbic acid. The reaction mixture was purged with N<sub>2</sub> and stirred for 16 h in an N<sub>2</sub> atmosphere. The product was purified using a Vivaspin membrane with a molecular weight cutoff of 10 kDa

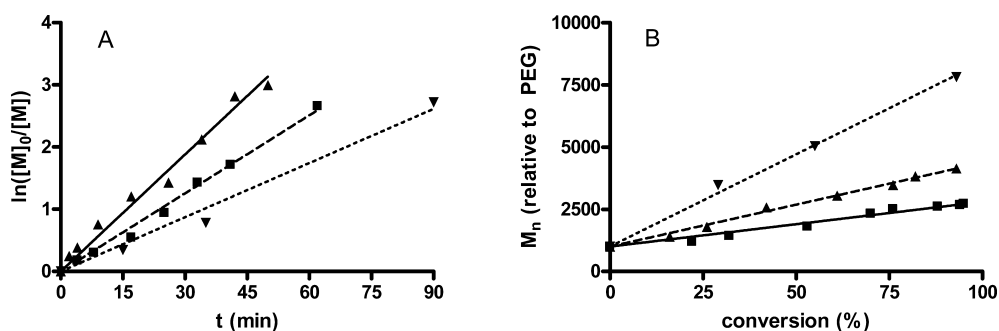


**Figure 1.** ATRP of OEGMA<sub>300</sub> using the synthesized peptide macroinitiator **5**: (A) semilogarithmic plot of monomer concentration  $[M]$  (as  $[M]_0/[M]$ ) in time; (B) number-averaged molecular weight  $M_n$  (determined by GPC) as a function of monomer conversion. (▲) target  $M_n = 4$  kDa, (■) target  $M_n = 8$  kDa, (▼) target  $M_n = 16$  kDa.

( $3 \times 10$ -fold concentration, each time diluting with H<sub>2</sub>O). Labeling of the polymer was verified by GPC using a MesoPore column (Polymer Laboratories) at 40 °C, with DMF + 10 mM LiCl as the eluent and both refractive index (RI) and fluorescence detection.

**Enzymatic Degradation.** Metalloprotease (type IV collagenase) from *C. Histolyticum* was used as a model for MMP-2 and MMP-9. This enzyme has very similar substrate specificity and is commonly used as a readily available alternative to MMP-2 and MMP-9.<sup>3,4</sup> The activity of the enzyme was determined colorimetrically by the *N*-(3-[2-furyl]acryloyl)-Leu-Gly-Pro-Ala (FALGPA) cleavage assay according to the manufacturer's protocol (Sigma-Aldrich) and was found to be 2300 units/mg (1 unit represents an activity of 1000 pmol substrate/min). The fluorescently labeled polymer was diluted to a final polymer concentration of 10  $\mu$ M in 0.22  $\mu$ m-filtered HEPES buffer of pH 7.4 containing 20 mM CaCl<sub>2</sub> and 100 mM NaCl at room temperature. Then, a solution (0.22  $\mu$ m-filtered) of 1000 units/mL of type IV collagenase in the same buffer was added to a final enzyme concentration of 10 units/mL, and the solution was incubated for 24 h at room temperature. GPC analysis with fluorescence detection was performed before and after the degradation (MesoPore column at 40 °C, DMF + 10 mM LiCl).

For the enzymatic degradation of intact micelles, micelles were formed by the above-mentioned heat shock procedure in HEPES buffer after which they were incubated with collagenase at 37 °C. At  $t = 0$  and after 24 h a sample was diluted 10-fold in preheated buffer and injected into a Nanosight LM10-HS laser light scattering/fluorescence microscopy system, preheated to 37 °C. Using the Nanoparticle Tracking Analysis (NTA) software, images were taken to visualize the micelles and to determine whether their fluorescently labeled coronas had been cleaved off.

## RESULTS AND DISCUSSION

**Functionalization of the Peptide C-Terminus.** To activate selectively the C-terminus of the peptide **3**, a reactive homoserine lactone was introduced by reaction of the penultimate methionine residue with CNBr (Scheme 3). This method, which is commonly used for the cleavage of recombinantly produced peptides from a carrier fusion protein,<sup>41</sup> allows for rapid and selective modification of the C-terminus of any peptide having methionine as the penultimate residue on the C-terminus.<sup>39,40</sup> The only requirement is the absence of internal methionine residues, which would lead to cleavage of the peptide. However, since methionine is one of the least occurring amino acids in proteins,<sup>47</sup> this requirement is often easy to meet, making methionine a favorable target for site-specific peptide conjugation. The main advantage over other methodologies that target the C-terminus, e.g., carbodiimide-based coupling,<sup>48</sup> is that CNBr functionalization is compatible with the presence of glutamate and aspartate residues. After reaction of the

peptide with excess cyanogen bromide, 95% of the peptide was converted into the lactone form **4** (HPLC). Apart from the small amount of unreacted peptide, there was also a trace impurity (<5%) of peptide in which the methionine residue had been oxidized to methionine sulfoxide, which renders it insensitive to lactonization with CNBr. The lactonized peptide was used without purification, as the main impurities are not reactive in the step of coupling the linker and could be removed after that step.

Linker **1**, which consists of a primary amine on one side and an efficient 2-bromoisobutyrate ATRP initiator on the other side, was synthesized in good yield and coupled to the peptide (Scheme 3). To catalyze aminolysis of the lactone, 10 mol % of 2-hydroxypyridine was added.<sup>49</sup> Nonreacted linker was easily removed after the reaction with the peptide, by selective precipitation, allowing the use of a large excess of linker. This yields a very short reaction time and negligible inter- and intramolecular reaction with the N-terminal amine. HPLC showed that after 15 min ~95% of the peptide lactone had reacted. After preparative HPLC, the peptide macroinitiator **5** was obtained in 73% yield.

**ATRP of OEGMA<sub>300</sub> Starting from the C-Terminus.** The polymerization of OEGMA<sub>300</sub> yields brush-shaped PEG-like polymers which are frequently used as hydrophilic polymers in the biomedical field since they possess several of the advantages over the well-known PEG, e.g., the fact that they are polymerizable by controlled radical polymerization.<sup>50–53</sup> Furthermore, because of the hydrophilic oligo(ethylene glycol) side chains and the hydrophobic polymethacrylate backbone, pOEGMA's have thermosensitive properties, which can be tuned by the average length of the oligo(ethylene glycol) side chains.<sup>53</sup> By using a monomer with an average molar mass of 300 Da, it was ensured that the resulting polymer has a lower critical solution temperature (LCST) above 68 °C,<sup>52</sup> meaning that the polymer is water-soluble at physiological temperature.

For the polymerization, a mild method compatible with the peptide was developed. Generally, ATRP of OEGMA is performed in alcohols at elevated temperatures,<sup>51,53</sup> but it can also be performed in aqueous media at room temperature.<sup>50</sup> By addition of Cu(II) and a small amount of CH<sub>3</sub>CN, a pseudoligand for Cu(I), the problem of disproportionation commonly faced in aqueous ATRP was eliminated.<sup>54,55</sup> Furthermore, by varying the percentage CH<sub>3</sub>CN (and consequently the polarity of the solvent), it is possible to adjust the rate of the reaction.<sup>56</sup> In the present study, a fast reaction with sufficient control at ambient temperature was obtained in a CH<sub>3</sub>CN/H<sub>2</sub>O 3/7 (v/v) solvent mixture, which is

a good solvent for the peptide used in the present study. As can be seen in Figure 1A, the residual monomer concentration decreased exponentially in time during the course of the reaction. This indicates a constant concentration of propagating radicals during the polymerization and thus effective and instantaneous initiation as well as negligible termination/combination; both are prerequisites for a controlled/living polymerization.<sup>57</sup> Furthermore, the number-averaged molecular weight ( $M_n$ ) evolved linearly with conversion (Figure 1B), indicating a low rate of termination. These observations indicate that the polymerization was controlled.

<sup>1</sup>H NMR spectroscopy of the polymers after purification showed that the pOEGMA blocks had  $M_n$  values of 3.2, 7.1, and 15.7 kDa, which are in good agreement with the expected molecular weights.

**Inactivation of the Living Chain-End.** One feature of ATRP is that the living chain end of the resulting polymers is able to reinitiate another polymerization, and this feature has been frequently used for the synthesis of block copolymers.<sup>58–61</sup> To be able to grow a different polymer chain from the other (N-) terminus of the peptide, however, it must be ensured that the already existing polymer chain on the C-terminus will not reinitiate in a subsequent ATRP. Therefore, the chloride on the living chain end was substituted by azide using a recently developed copper-catalyzed azide substitution reaction.<sup>42</sup> The introduced azide functionality also renders it possible to attach in a later stage a fluorescent probe or a targeting ligand using azide/alkyne “click” chemistry.<sup>42,62–68</sup> Figure 2 shows that the substitution with  $\text{NaN}_3$ , as expected,

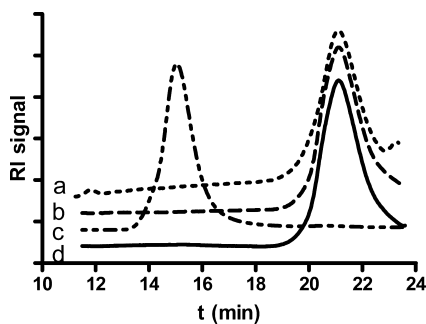


**Figure 2.** GPC chromatograms of peptide-pOEGMA<sub>4</sub> kDa hybrid polymer: (a) before substitution of the chloride chain end with azide, (b) after substitution with azide, (c) non-azidated polymer after chain extension with NIPAm, and (d) azidated polymer after chain extension.

did not alter the molecular weight (distribution) of the polymer as determined by GPC analysis. Furthermore, the non-substituted pOEGMA chain could be extended with a pNIPAm block, which provides indeed evidence for the living character of the ATRP of OEGMA on the peptide macroinitiator. On the other hand, after substitution with  $\text{NaN}_3$ , pOEGMA was not able to reinitiate an ATRP (Figure 2). This demonstrates quantitative substitution of the Cl end-group by azide.

**Functionalization of the N-Terminus.** Introduction of an aldehyde functionality into a peptide by mild periodate oxidation of an N-terminal serine residue followed by coupling of an O-substituted hydroxylamine is a highly selective, efficient, and well-known bioconjugation reaction.<sup>69–71</sup> The formed oxime bonds are acid-sensitive but stable at physiological pH.<sup>72</sup> The peptide-pOEGMA conjugates **6** were subjected to the above-mentioned oxidation with  $\text{NaIO}_4$  in

phosphate buffer (pH 7.4) (Scheme 4). Reaction with fluorescamine indicated disappearance of the amine functionality of the N-terminal serine. Furthermore, a sample taken from the reaction mixture developed a yellow color after addition of 2,4-dinitrophenylhydrazine, indicating the formation of an aldehyde.

For further functionalization of the aldehyde-modified terminus of the peptide **7**, linker **2** was developed, carrying on one side a reactive aminoxy group and on the other side an ATRP initiator functionality. Linker **2** was synthesized as shown in Scheme 2. Subsequently, the aldehyde-functionalized peptide-pOEGMA conjugates **7** were incubated with linker **2** in 50 mM anilinium acetate buffer (pH 4.6) (Scheme 4), a known catalyst for the formation of oxime bonds.<sup>71,73,74</sup> After coupling of linker **2**, the appearance of a peak at  $\delta$  7.7 ppm in <sup>1</sup>H NMR (in  $\text{D}_2\text{O}$ ) indicated the formation of an oxime bond (Figure 3).

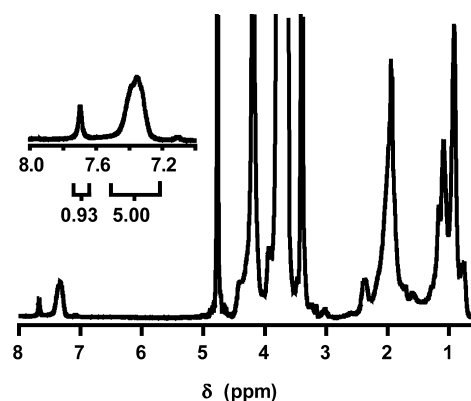


**Figure 3.** NMR spectrum of linker 2-peptide-pOEGMA<sub>4</sub> kDa showing the peak of the proton on the oxime carbon at  $\delta$  7.7 ppm and the aromatic phenylalanine protons at  $\delta$  7.3–7.4 ppm.

The degree of functionalization was >90% based on comparison of the integral of this peak with the integral of the peak of the phenyl protons of phenylalanine ( $\delta$  7.5–7.2 ppm).

**ATRP of the N-Terminal Block.** NIPAm was polymerized from the modified N-terminus of the peptide-pOEGMA conjugates **8** by ATRP in a  $\text{CH}_3\text{CN}/\text{H}_2\text{O}$  3/7 (v/v) mixture at 0 °C.<sup>44,56,75</sup> The reaction was well controlled as evidenced by an exponential decrease of the residual monomer concentration (Figure 4A) and a linear evolution of  $M_n$  with conversion, for both target molecular weights of the pNIPAm block (Figure 4B). This indicates successful growth of the pNIPAm block, starting from the peptide-pOEGMA macroinitiator **8**.

**Characterization of the Polymers and Their Micelles.** The structure of the final polymers is depicted in Figure 5. <sup>1</sup>H NMR analysis showed that the pNIPAm blocks had  $M_n$  values in good agreement with the expected molecular weight, based on the comparison of the integrals of the pOEGMA methoxy protons and pNIPAm methyl protons (Table 1). Furthermore, the dispersity of the synthesized polymers was low, with only polymers containing a pOEGMA<sub>16</sub> kDa block having a somewhat broader size distribution.

The cmc of the polymers dissolved in water was equal for all polymers. In general, a decrease in cmc with increasing hydrophobic block length would be expected, as well as an increase in cmc with increasing hydrophilic block length.<sup>76,77</sup> Our observation of equal cmc's might be related to the fact that

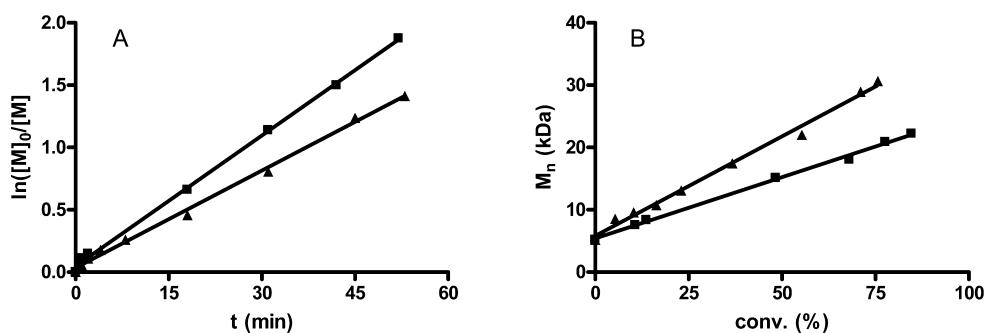


**Figure 4.** Kinetics of the polymerization of NIPAm onto peptide-pOEGMA<sub>8</sub> kDa: (A) semilogarithmic plot of monomer concentration  $[M]$  (as  $[M]_0/[M]$ ) in time; (B) number-averaged molecular weight  $M_n$  as a function of monomer conversion. (■) Target  $M_n = 16$  kDa, (▲) target  $M_n = 32$  kDa.

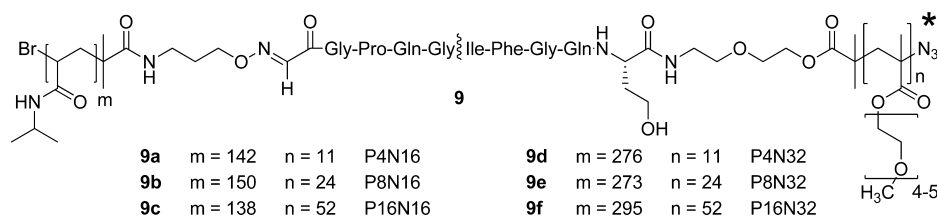


**Figure 5.** Structure of the final biohybrid triblock polymers. The wavy line indicates the bond that is cleavable by MMPs. The asterisk indicates the attachment point of the fluorescent probe in the P8N32 polymer.

**Table 1.** Properties of the Polymers and Their Micelles

abbrev <sup>a</sup>	polymers			micelles				
	$M_n^b$ (kDa)		$D^c$	CP <sup>d</sup> (°C)		cmc <sup>e</sup> (mg/mL)	$R_h^f$ (nm) (PDI)	
	pOEGMA	pNIPAm		H <sub>2</sub> O	PBS		H <sub>2</sub> O	PBS
P4	3.2		1.20					
P4N16	3.2	16.0	1.25	35.5 ± 0.1	33.0 ± 0.2	0.03 ± 0.01	29 ± 1 (0.1)	173 ± 2 (0.1)
P4N32	3.2	31.2	1.24	34.5 ± 0.1	32.0 ± 0.2	0.03 ± 0.01	28 ± 1 (0.1)	1756 ± 138 (0.5)
P8	7.1		1.32					
P8N16	7.1	17.0	1.24	35.6 ± 0.1	33.1 ± 0.1	0.03 ± 0.01	27 ± 1 (0.1)	35 ± 1 (0.1)
P8N32	7.1	30.8	1.26	34.8 ± 0.1	32.2 ± 0.1	0.03 ± 0.01	27 ± 1 (0.1)	123 ± 2 (0.1)
P16	15.7		1.45					
P16N16	15.7	15.6	1.52	36.0 ± 0.1	33.2 ± 0.1	0.03 ± 0.01	23 ± 1 (0.2)	24 ± 1 (0.1)
P16N32	15.7	33.3	1.64	34.7 ± 0.1	32.1 ± 0.1	0.03 ± 0.01	22 ± 1 (0.1)	33 ± 1 (0.1)

<sup>a</sup>P denotes the aimed size of the pOEGMA block and N that of the pNIPAm block (both in kDa). <sup>b</sup>Number-averaged molecular weight based on <sup>1</sup>H NMR. <sup>c</sup>Dispersity from GPC. <sup>d</sup>Cloud point. <sup>e</sup>Critical micelle concentration. <sup>f</sup>Z-averaged hydrodynamic radius ( $R_h$ ) from DLS.

the found cmc values are very low, permitting an influence from the fluorescent probe (pyrene) itself.<sup>78</sup>

The CPs of the polymers dissolved in water were slightly higher than the published value of 32 °C of pNIPAm homopolymer in water due to the presence of large hydrophilic polymer blocks.<sup>79,80</sup>

Consequently, Table 1 shows that the CP in water increased from 35.5 to 36.0 °C with increasing the pOEGMA block length from 4 to 16 kDa (P4N16 vs P16N16) and decreased with increasing the pNIPAm length from 16 to 32 kDa. For self-assembly into micelles, a heat-shock protocol was used as it has been described that instantaneous heating of aqueous polymer solutions to above their CP leads to well-defined micelles.<sup>46</sup> Following this procedure, all polymers formed micelles with a size of 22–29 nm in water and narrow size distributions, which is favorable for drug delivery purposes.<sup>81</sup>

Increasing the pOEGMA length from 4 to 16 kDa leads to a larger surface area that is needed per polymer chain and thus to less polymer chains fitting in one micelle:<sup>44</sup> consequently, the size of the micelles decreased from 29 nm (P4N16) to 23 nm

(P16N16). Interestingly, increasing the pNIPAm block from 16 to 32 kDa did not lead to an increase of the micellar size, but to a small decrease, e.g., 29 nm (P4N16) vs 28 nm (P4N32). This effect has been observed before and has been attributed to greater hydrophobicity of the longer pNIPAm blocks, leading to more extensive dehydration of the micellar cores.<sup>46,82</sup>

The difference in CP and size between micelles dispersed in water and PBS is also striking. The salting-out effect of PBS reduced the CPs by 2–3 °C, to values (32–33 °C) that are well below physiological temperature and thus compatible with drug delivery applications. Furthermore, PBS also led to a higher observed Z-averaged size. PEG is known to partially dehydrate upon addition of salt,<sup>46,83,84</sup> and the same behavior may be expected for pOEGMA. This partial dehydration may lead to the formation of larger particles due to a change in the ratio between the hydrodynamic volumes of the hydrophilic and hydrophobic blocks. For large pOEGMA blocks and/or small pNIPAm blocks, the hydrophilic/hydrophobic ratio in buffer is still enough to form small micelles (P8N16, P16N16, and P16N32); for smaller pOEGMA blocks, the increase in size was

more pronounced. For the P4N32 polymer, the (decreased) hydrodynamic volume of the pOEGMA blocks in buffer was not enough anymore to support stable nanoparticles, and aggregation resulted.

**Enzymatic Degradation.** The peptide separating the hydrophilic micelle corona from the thermosensitive micelle core has been designed to be cleaved by MMP-2 and MMP-9, as these enzymes are upregulated in diseased tissues (e.g., in cancer and rheumatoid arthritis). For this reason, MMP-2/MMP-9 substrates have previously been utilized as building blocks of tissue-specific drug delivery systems.<sup>85–90</sup>

To verify that the peptide could still be cleaved by metalloproteases after growing the two polymer blocks on its N- and C-termini, the P8N32 block copolymer was fluorescently labeled at the end of its hydrophilic block. Alkyne-functionalized Alexa Fluor 555 was coupled (“clicked”) to the azide-functionalized chain end by Cu(I)-catalyzed azide–alkyne cycloaddition. A label to polymer molar ratio of 1:10 was used in order to minimize any effects of the label on micelle formation. As shown in Figure 6, the polymer was successfully labeled with Alexa Fluor 555 by this procedure.

Subsequently, the polymer was incubated with collagenase for 24 h at room temperature. The cleaved polymer was then

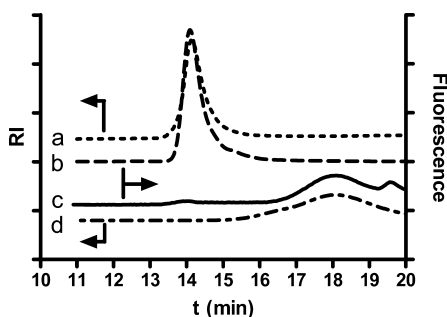


**Figure 6.** GPC traces of the fluorescently labeled polymer: (a) RI signal after labeling, (b) fluorescence signal ( $\lambda_{\text{ex}} = 555 \text{ nm}$ ,  $\lambda_{\text{em}} = 585 \text{ nm}$ ) after labeling, (c) fluorescence signal after enzymatic cleavage. For comparison, (d) shows the RI signal of peptide-pOEGMA<sub>8</sub> kDa.

analyzed by GPC with fluorescence detection. It is well-known that pNIPAm (co)polymers elute in GPC at retention times corresponding to much higher molecular weights than expected, probably due to very persistent interchain hydrogen bonds.<sup>91,92</sup> This feature was exploited for the demonstration of cleavage of the peptide–polymer conjugate by collagenase. When a column with a narrow separation range was used, the fluorescently labeled intact polymer elutes in the void volume (at 14 min, Figure 6), whereas the fluorescently labeled pOEGMA that is cleaved off elutes much later (at 18 min, the same retention time as peptide-pOEGMA<sub>8</sub> kDa). Since the pNIPAm is unlabeled after cleavage, it is invisible using fluorescence detection. Thus, this method leads to a good separation of the uncleaved polymer and the cleaved-off hydrophilic blocks, while preventing interference from the cleaved thermosensitive blocks which coelute with the uncleaved polymer but are invisible using fluorescence detection.

To visualize the enzymatic degradation of the particles, micelles were formed by heat-shocking the fluorescently labeled polymer. Images of the solution were taken using a preheated Nanosight LM10-HS microscopy system which allows visualization of the nanoparticles by either their scattering of laser

light or by their fluorescence. Images were obtained in both laser scattering and fluorescence mode directly before addition of the enzyme and after 24 h incubation at 37 °C (Figure 7). As can be seen in Figure 7C, particles are still present after degradation, but their fluorescence has vanished into the

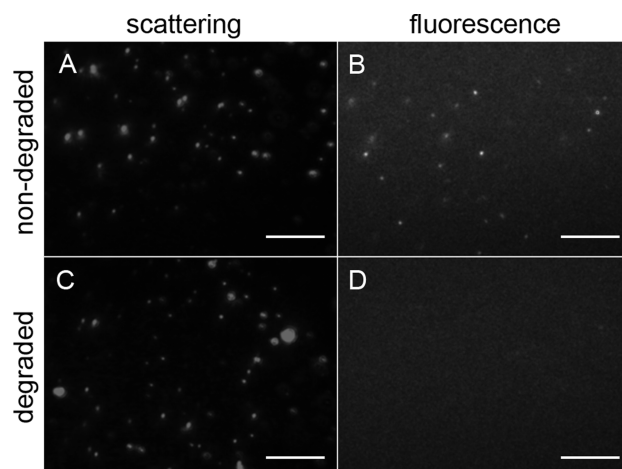


**Figure 7.** Images of the micellar dispersion of fluorescently labeled P8N32 polymer, taken using a Nanosight system before (A and B) and after (C and D) enzymatic cleavage in HEPES buffer. (A) and (C) were recorded in scattering mode and (B) and (D) in fluorescence mode ( $\lambda_{\text{ex}} = 532 \text{ nm}$ ,  $\lambda_{\text{em}} > 565 \text{ nm}$ ), keeping the camera gain settings constant. Scale bars correspond to 10  $\mu\text{m}$ ; however, the apparent size of the micelles in these images reflects their scattering intensity rather than their actual size.

background noise (Figure 7D), indicating that the fluorescent and highly mobile hydrophilic pOEGMA chains have been cleaved off by the enzyme. On the basis of these findings, it can be expected that when these micelles are used for drug delivery to tumors or inflamed tissues, their “stealth” corona will be cleaved off at the target site of action. We hypothesize that this “shedding” of the corona will impede further circulation of the micelles and facilitate cellular uptake.

## CONCLUSION

We have demonstrated a suitable approach to grow two different polymer chains from a native peptide by ATRP, using two orthogonal methods to couple ATRP initiators to the N- and C-terminus. Furthermore, in this work a mild method is presented to inactivate the first living ATRP chain end, allowing the same polymerization chemistry for both polymerizations. Both polymerizations were well controlled, leading to a well-defined end product with control over the desired polymer block lengths.

Above the cloud point of one of the blocks, the polymers self-assembled into micelles. The micelles have been shown to “shed” the hydrophilic polymer blocks on their outside by the action of collagenase, a model for diseased tissue-specific matrix metalloproteases. Thus, the technology presented herein offers new possibilities for enzyme-triggered drug delivery.

## AUTHOR INFORMATION

### Corresponding Author

\*E-mail: w.e.hennink@uu.nl.

## ■ REFERENCES

- (1) Ruiz-Hitzky, E.; Darder, M.; Aranda, P.; Ariga, K. *Adv. Mater.* **2010**, *3*, 323–336.
- (2) Venkatesh, S.; Byrne, M. E.; Peppas, N. A.; Hilt, J. Z. *Expert Opin. Drug Delivery* **2005**, *6*, 1085–1096.
- (3) Tsurkan, M. V.; Chwalek, K.; Levental, K. R.; Freudenberg, U.; Werner, C. *Macromol. Rapid Commun.* **2010**, *17*, 1529–1533.
- (4) Seliktar, D.; Zisch, A. H.; Lutolf, M. P.; Wrana, J. L.; Hubbell, J. A. *J. Biomed. Mater. Res., Part A* **2004**, *4*, 704–716.
- (5) Fuks, G.; Mayap Talom, R.; Gauffre, F. *Chem. Soc. Rev.* **2011**, *5*, 2475–2493.
- (6) Xun, W.; Wu, D. Q.; Li, Z. Y.; Wang, H. Y.; Huang, F. W.; Cheng, S. X.; Zhang, X. Z.; Zhuo, R. X. *Macromol. Biosci.* **2009**, *12*, 1219–1226.
- (7) Habraken, G. J.; Peeters, M.; Thornton, P. D.; Koning, C. E.; Heise, A. *Biomacromolecules* **2011**, *12*, 3761–3769.
- (8) Oerlemans, C.; Bult, W.; Bos, M.; Storm, G.; Nijssen, J. F. W.; Hennink, W. E. *Pharm. Res.* **2010**, *27*, 2569–2589.
- (9) Glinel, K.; Jonas, A. M.; Jouenne, T.; Leprince, J.; Galas, L.; Huck, W. T. *Bioconjugate Chem.* **2009**, *1*, 71–77.
- (10) Ku, T.; Chien, M.; Thompson, M. P.; Sinkovits, R. S.; Olson, N. H.; Baker, T. S.; Gianneschi, N. C. *J. Am. Chem. Soc.* **2011**, *22*, 8392–8395.
- (11) Bencherif, S. A.; Gao, H.; Srinivasan, A.; Siegwart, D. J.; Hollinger, J. O.; Washburn, N. R.; Matyjaszewski, K. *Biomacromolecules* **2009**, *7*, 1795–1803.
- (12) Katayama, Y.; Sonoda, T.; Maeda, M. *Macromolecules* **2001**, *24*, 8569–8573.
- (13) Zhu, B.; Lu, D.; Ge, J.; Liu, Z. *Acta Biomater.* **2011**, *5*, 2131–2138.
- (14) Broyer, R. M.; Quaker, G. M.; Maynard, H. D. *J. Am. Chem. Soc.* **2007**, *3*, 1041–1047.
- (15) Pintauer, T.; Matyjaszewski, K. *Chem. Soc. Rev.* **2008**, *6*, 1087–1097.
- (16) Fristrup, C. J.; Jankova, K.; Hvilsted, S. *Soft Matter* **2009**, *23*, 4623–4634.
- (17) Min, K.; Matyjaszewski, K. *Cent. Eur. J. Chem.* **2009**, *4*, 657–674.
- (18) Boyer, C.; Bulmus, V.; Davis, T. P.; Admiral, V.; Liu, J.; Perrier, S. *Chem. Rev.* **2009**, *11*, 5402–5436.
- (19) Gregory, A.; Stenzel, M. H. *Expert Opin. Drug Delivery* **2011**, *2*, 237–269.
- (20) Stenzel, M. H. *Chem. Commun. (Cambridge, U. K.)* **2008**, *30*, 3486–3503.
- (21) Studer, A.; Schulte, T. *Chem. Rec.* **2005**, *1*, 27–35.
- (22) Brinks, M. K.; Studer, A. *Macromol. Rapid Commun.* **2009**, *13*, 1043–1057.
- (23) Bertin, D.; Gigmes, D.; Marque, S. R. A.; Tordo, P. *Chem. Soc. Rev.* **2011**, *5*, 2189–2198.
- (24) Braunecker, W. A.; Matyjaszewski, K. *Prog. Polym. Sci.* **2007**, *1*, 93–146.
- (25) Grover, G. N.; Maynard, H. D. *Curr. Opin. Chem. Biol.* **2010**, *6*, 818–827.
- (26) Topp, M. D. C.; Dijkstra, P. J.; Talsma, H.; Feijen, J. *Macromolecules* **1997**, *30*, 8518–8520.
- (27) Neradovic, D.; van Nostrum, C. F.; Hennink, W. E. *Macromolecules* **2001**, *34*, 7589–7591.
- (28) Netzel-Arnett, S.; Sang, Q. X.; Moore, W. G.; Navre, M.; Birkedal-Hansen, H.; Van Wart, H. E. *Biochemistry* **1993**, *25*, 6427–6432.
- (29) Benassi, M. S.; Gamberi, G.; Magagnoli, G.; Molendini, L.; Ragazzini, P.; Merli, M.; Chiesa, F.; Ballardelli, A.; Manfrini, M.; Bertoni, F.; Mercuri, M.; Picci, P. *Ann. Oncol.* **2001**, *1*, 75–80.
- (30) Raithatha, S. A.; Muzik, H.; Muzik, H.; Rewcastle, N. B.; Johnston, R. N.; Edwards, D. R.; Forsyth, P. A. *Neuro-Oncology (Cary, NC, U. S.)* **2000**, *3*, 145–150.
- (31) Kevorkian, L.; Young, D. A.; Darrach, C.; Donell, S. T.; Shepstone, L.; Porter, S.; Brockbank, S. M.; Edwards, D. R.; Parker, A. E.; Clark, I. M. *Arthritis Rheum.* **2004**, *1*, 131–141.
- (32) Maeda, H.; Wu, J.; Sawa, T.; Matsumura, Y.; Hori, K. *J. Controlled Release* **2000**, *1–2*, 271–284.
- (33) Khorsand Sourkahi, B.; Cunningham, A.; Zhang, Q.; Oh, J. K. *Biomacromolecules* **2011**.
- (34) Habraken, G. J. M.; Koning, C. E.; Heise, A. *J. Polym. Sci., Part A: Polym. Chem.* **2009**, *24*, 6883–6893.
- (35) Sun, P.; Zhang, Y.; Shi, L.; Gan, Z. *Macromol. Biosci.* **2010**, *6*, 621–631.
- (36) Ciampolini, M.; Nardi, N. *Inorg. Chem.* **1966**, *1*, 41–44.
- (37) Salisbury, C. M.; Maly, D. J.; Ellman, J. A. *J. Am. Chem. Soc.* **2002**, *50*, 14868–14870.
- (38) Chan, W. C., White, P. D., Eds.; *Fmoc Solid Phase Peptide Synthesis: A Practical Approach*; Oxford University Press: New York, 2000.
- (39) Marcus, J. H. *Anal. Biochem.* **1975**, *2*, 583–589.
- (40) Horn, M. J.; Laursen, R. A. *FEBS Lett.* **1973**, *3*, 285–288.
- (41) LaVallie, E. R.; McCoy, J. M.; Smith, D. B.; Riggs, P. *Enzymatic and Chemical Cleavage of Fusion Proteins. In Current Protocols in Molecular Biology*; John Wiley & Sons, Inc.: New York, 2001.
- (42) de Graaf, A. J.; Mastrobattista, E.; Van Nostrum, C. F.; Rijkers, D. T. S.; Hennink, W. E.; Vermonden, T. *Chem. Commun. (Cambridge, U. K.)* **2011**, *24*, 6972–6974.
- (43) Dirksen, A.; Dirksen, S.; Hackeng, T. M.; Dawson, P. E. *J. Am. Chem. Soc.* **2006**, *49*, 15602–15603.
- (44) de Graaf, A. J.; Boere, K. W. M.; Kemmink, J.; Fokink, R. G.; van Nostrum, C. F.; Rijkers, D. T. S.; van, d. G.; Wienk, H.; Baldus, M.; Mastrobattista, E.; Vermonden, T.; Hennink, W. E. *Langmuir* **2011**, *16*, 9843–9848.
- (45) Wilhelm, M.; Zhao, C. L.; Wang, Y.; Xu, R.; Winnik, M. A.; Mura, J. L.; Riess, G.; Croucher, M. D. *Macromolecules* **1991**, *5*, 1033–1040.
- (46) Neradovic, D.; Soga, O.; Van Nostrum, C. F.; Hennink, W. E. *Biomaterials* **2004**, *12*, 2409–2418.
- (47) Wu, G.; Ott, T. L.; Knabe, D. A.; Bazer, F. W. *J. Nutr.* **1999**, *5*, 1031–1038.
- (48) Valeur, E.; Bradley, M. *Chem. Soc. Rev.* **2009**, *2*, 606–631.
- (49) Openshaw, H. T.; Whittaker, N. *J. Chem. Soc. C* **1969**, *1*, 89–91.
- (50) Wang, X.; Armes, S. P. *Macromolecules* **2000**, *18*, 6640–6647.
- (51) Lutz, J.-F.; Hoth, A. *Macromolecules* **2006**, *2*, 893–896.
- (52) Ishizone, T.; Seki, A.; Hagiwara, M.; Han, S.; Yokoyama, H.; Oyane, A.; Deffieux, A.; Carlotti, S. *Macromolecules* **2008**, *8*, 2963–2967.
- (53) Badi, N.; Lutz, J.-F. *J. Controlled Release* **2009**, *3*, 224–229.
- (54) Tsarevsky, N. V.; Braunecker, W. A.; Matyjaszewski, K. *J. Organomet. Chem.* **2007**, *15*, 3212–3222.
- (55) Tsarevsky, N. V.; Matyjaszewski, K. *Chem. Rev.* **2007**, *6*, 2270–2299.
- (56) Ye, J.; Narain, R. *J. Phys. Chem. B* **2009**, *3*, 676–681.
- (57) Matyjaszewski, K. *Curr. Opin. Solid State Mater. Sci.* **1996**, *6*, 769–776.
- (58) Shipp, D. A.; Wang, J.; Matyjaszewski, K. *Macromolecules* **1998**, *23*, 8005–8008.
- (59) Ma, Q.; Wooley, K. L. *J. Polym. Sci., Part A* **2000**, No. Suppl., 4805–4820.
- (60) Davis, K. A.; Matyjaszewski, K. *Macromolecules* **2000**, *11*, 4039–4047.
- (61) Liu, S.; Weaver, J. V. M.; Tang, Y.; Billingham, N. C.; Armes, S. P.; Tribe, K. *Macromolecules* **2002**, *16*, 6121–6131.
- (62) Tornøe, C. W.; Christensen, C.; Meldal, M. *J. Org. Chem.* **2002**, *9*, 3057–3064.
- (63) Rostovtsev, V. V.; Green, L. G.; Fokin, V. V.; Sharpless, K. B. *Angew. Chem., Int. Ed.* **2002**, *14*, 2596–2599.
- (64) Meldal, M.; Tornøe, C. W. *Chem. Rev.* **2008**, *8*, 2952–3015.
- (65) Lutz, J.-F. *Angew. Chem., Int. Ed.* **2007**, *7*, 1018–1025.
- (66) Binder, W. H.; Sachsenhofer, R. *Macromol. Rapid Commun.* **2007**, *1*, 15–54.
- (67) Lutz, J.-F.; Börner, H. G.; Weichenhan, K. *Macromol. Rapid Commun.* **2005**, *7*, 514–518.

- (68) Lutz, J.-F.; Börner, H. G.; Weichenhan, K. *Macromolecules* **2006**, *19*, 6376–6383.
- (69) Gaertner, H. F.; Offord, R. E. *Bioconjugate Chem.* **1996**, *1*, 38–44.
- (70) Rose, K.; Chen, J.; Dragovic, M.; Zeng, W.; Jeannerat, D.; Kamalaprija, P.; Burger, U. *Bioconjugate Chem.* **1999**, *6*, 1038–1043.
- (71) Dirksen, A.; Hackeng, T. M.; Dawson, P. E. *Angew. Chem., Int. Ed.* **2006**, *45*, 7581–7584.
- (72) Jin, Y.; Song, L.; Su, Y.; Zhu, L.; Pang, Y.; Qiu, F.; Tong, G.; Yan, D.; Zhu, B.; Zhu, X. *Biomacromolecules* **2011**, *10*, 3460–3468.
- (73) Dirksen, A.; Dawson, P. E. *Bioconjugate Chem.* **2008**, *12*, 2543–2548.
- (74) Thygesen, M. B.; Munch, H.; Sauer, J.; Cló, E.; Jørgensen, M. R.; Hindsgaul, O.; Jensen, K. J. *J. Org. Chem.* **2010**, *5*, 1752–1755.
- (75) Millard, P. E.; Mougin, N. C.; Böker, A.; Müller, A. H. E. *Polym. Prepr. (Am. Chem. Soc., Div. Polym. Chem.)* **2008**, *49*, 121–122.
- (76) van Hell, A. J.; Costa, C. I. C. A.; Flesch, F. M.; Sutter, M.; Jiskoot, W.; Crommelin, D. J. A.; Hennink, W. E.; Mastrobattista, E. *Biomacromolecules* **2007**, *9*, 2753–2761.
- (77) Carstens, M. G.; van Nostrum, C. F.; Ramzi, A.; Meeldijk, J. D.; Verrijck, R.; de Leede, L. L.; Crommelin, D. J.; Hennink, W. E. *Langmuir* **2005**, *24*, 11446–11454.
- (78) Jones, G.; Vullev, V. I. *Org. Lett.* **2001**, *16*, 2457–2460.
- (79) Teodorescu, M.; Negru, I.; Stanescu, P. O.; Drăghici, C.; Lungu, A.; Sârbu, A. *React. Funct. Polym.* **2010**, *10*, 790–797.
- (80) Xia, Y.; Yin, X.; Burke, N. A. D.; Stöver, H. D. H. *Macromolecules* **2005**, *14*, 5937–5943.
- (81) Saha, R. N.; Vasanthakumar, S.; Bende, G.; Snehalatha, M. *Mol. Membr. Biol.* **2010**, *7*, 215–231.
- (82) Soga, O.; van Nostrum, C. F.; Ramzi, A.; Visser, T.; Soulimani, F.; Frederik, P. M.; Bomans, P. H. H.; Hennink, W. E. *Langmuir* **2004**, *21*, 9388–9395.
- (83) Louai, A.; Sarazin, D.; Pollet, G.; François, J.; Moreaux, F. *Polymer* **1991**, *4*, 713–720.
- (84) Govender, T.; Stolnik, S.; Xiong, C.; Zhang, S.; Illum, L.; Davis, S. S. J. *Controlled Release* **2001**, *3*, 249–258.
- (85) Yamada, R.; Kostova, M. B.; Anchoori, R. K.; Xu, S.; Neamati, N.; Khan, S. R. *Cancer Biol. Ther.* **2010**, *3*, 192–203.
- (86) Wong, C.; Stylianopoulos, T.; Cui, J.; Martin, J.; Chauhan, V. P.; Jiang, W.; Popovic, Z.; Jain, R. K.; Bawendi, M. G.; Fukumura, D. *Proc. Natl. Acad. Sci. U. S. A.* **2011**, *6*, 2426–2431.
- (87) Garripelli, V. K.; Kim, J.; Son, S.; Kim, W. J.; Repka, M. A.; Jo, S. *Acta Biomater.* **2011**, *5*, 1984–1992.
- (88) Kratz, F.; Dreves, J.; Bing, G.; Stockmar, C.; Scheuermann, K.; Lazar, P.; Unger, C. *Bioorg. Med. Chem. Lett.* **2001**, *15*, 2001–2006.
- (89) Atkinson, J. M.; Siller, C. S.; Gill, J. H. *Br. J. Pharmacol.* **2008**, *7*, 1344–1352.
- (90) Vartak, D. G.; Gemeinhart, R. A. *J. Drug Targeting* **2007**, *1*, 1–20.
- (91) Ganachaud, F.; Monteiro, M. J.; Gilbert, R. G.; Dourges, M.; Thang, S. H.; Rizzardo, E. *Macromolecules* **2000**, *18*, 6738–6745.
- (92) Smithenry, D. W.; Kang, M.; Gupta, V. K. *Macromolecules* **2001**, *24*, 8503–8511.